2

BNL-27114

MASTER

CONF-790219--12

PARAMETERS IN SEMI-EMPIRICAL THEORIES OF ALLOY PHASE FORMATION

by

L. H. Bennett
National Bureau of Standards
Washington, D. C. 20234

and

R. E. Watson+
Brookhaven National Laboratory
Upton, New York

DISCLAIMER

This book was prepared as an account of work sponsored by an agency of the United States Government. Neither the United States Government nor any agency thereof, nor any of their employees, makes any warranty, express or implied, or assumes any legal liability or responsibility for the accuracy, completeness, or usefulness of any information, apparatus, product, or process disclosed, or represents that its use would not infringe privately owned rights. Reference herein to any specific commercial product, process, or service by trade name, trademark, manufacturer, or otherwise, does not necessarily constitute or imply its endorsement, recommendation, or favoring by the United States Government or any agency thereof. The views and opinions of authors expressed herein do not necessarily state or reflect those of the United States Government or any agency thereof.

+ Research at Brookhaven National Laboratory supported by the Division of Basic Energy Sciences, U. S. Department ofEnergy, under Contract No. DE-AC02-76CH00016.

The submitted manuscript has been authored under contract DE-AC02-76CH00016 with the Division of Basic Energy Sciences, U.S. Department of Energy. Accordingly, the U.S. Government retains a nonexclusive, royalty-free license to publish or reproduce the published form of this contribution, or allow others to do so, for U.S. Government purposes.

DISTRIBUTION OF THIS DOCUMENT IS UNLIMITED

PARAMETERS IN SEMI-EMPIRICAL THEORIES OF ALLOY PHASE FORMATION

L. H. Bennett
National Bureau of Standards
Washington, D.C. 20234

and

R. E. Watson[+]
Brookhaven National Laboratory
Upton, New York

Many theories of alloy solubility, structural stability of compounds, and heats of formation in alloying rely on parameters such as valence, size or electronegativity for their predictions. Nature, of course, requires only one parameter, the nuclear charge, to completely specify all the electronic properties of the elements. Thus, the atomic parameters are, of necessity, intimately connected with one another. It is our object in this presentation to review the physical origins of some of the more popular parameters used. We will emphasize the relationship of the different electronegativity scales to each other, and the relationship of electronegativity to other parameters such as atomic size. Structural stability maps employing electronegativity and some other parameters are shown for intermetallic compounds formed from different classes of elements: main group-main group, transition metal-main group, and transition metal-transition metal.

[+]Consultant at the National Bureau of Standards.

I. Introduction

In these proceedings we see a variety of models, employing apparently different sets of physical parameters to describe various alloy properties. On the whole, each of the models enjoys at least modest success. But note that, neglecting isotopic mass effects, the chemical properties of an element derive from a single parameter, the nuclear charge. It would therefore seem that the different physical parameters, which are intuitively so useful in describing alloy properties, are closely related to one another. When devising his now-classic rules (1) of alloy formation, Hume-Rothery recognized that "independent" parameters such as electronegativity, size and valence are indeed not independent. For example, in first approximation, the electronegativity is solely a function of electron density, hence of the valence divided by atomic volume. Such a relationship can be seen in a 1946 plot (2) of Gordy's (Fig. 1) involving the noble and main group elements and a few of the lighter transition elements. A bond radius rather than a volume appears in the denominator and more will be said of this later.

There are times when, on physical or empirical grounds, one finds that one particular parameter is important to experimental trends. Packing considerations, involving the relative size of constituents, provides considerable insight (3) into the structures into which various compounds are formed. While the insights are, we believe, correct in this case, empirical rules can be misleading. Plots of the electronegativity and of the inverse of atomic size map one another quite well across much of the periodic table as can be seen in Fig. 2. Thus some property depending on size might be correlated with the electronegativity or vice versa. The heats of formation of the chlorides and the compressibilities of the elements look much alike, Fig. 3, and while we believe the former to depend primarily on electronegativity and the latter on valence electron density a numerical correlation can, in fact, be made between the compressibilities and electronegativity values.

More often than not it is necessary to introduce more than one of the interrelated parameters when describing physical trends: size and electronegativity enter the Darken-Gurry plots of alloy solubility described by Gschneidner in his memorial (4) to Larry Darken at the start of this symposium and we have seen (5) Miedema employ electronegativity, electron density, and, to a weaker extent, size, in his description of compound heats of formation (6).

Not only are we forced to use a set of non-independent parameters but it often proves useful to allow one parameter to modify another. Pauling introduced (7) the effect of electronegativity, ϕ, on a bond length, D with the relationship

$$D(A-B) = r_A + r_B - C\,|\phi_A - \phi_B| \qquad (1)$$

TABLE I

The Valence of Copper

Chemical (Cuprous and Cupric)	1,2
Hume-Rothery e/a	1
Pauling	5.56
Engel-Brewer	2.75

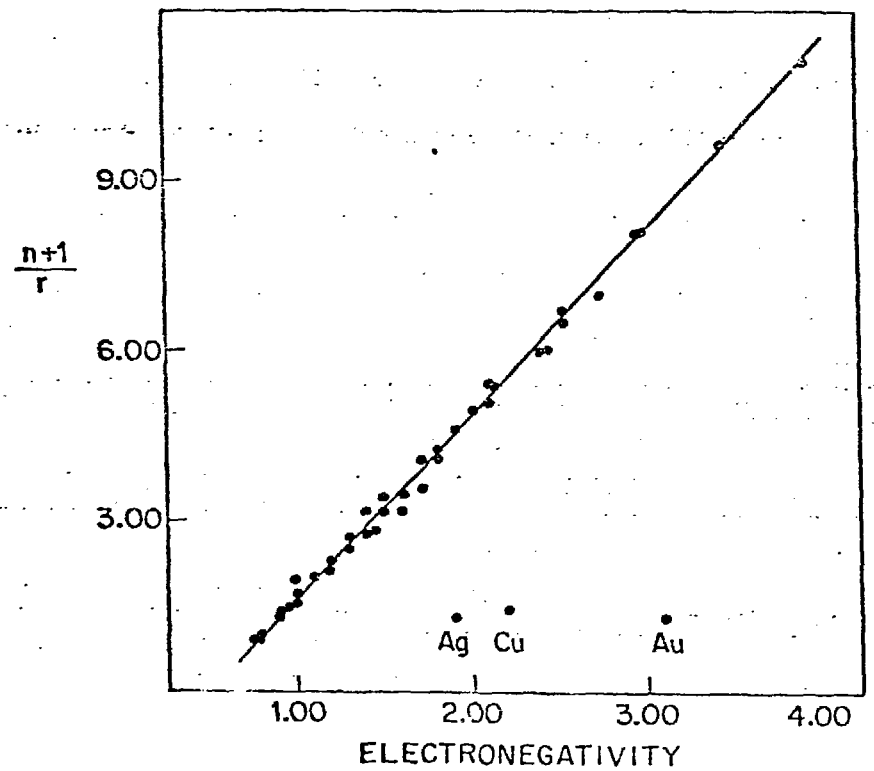

Fig. 1 - Gordy plot relating valence, radius, and Pauling electronegativity for a large number of elements. r is the single-bond covalent radius and n the number of valence electrons. Note that the nearly-filled d-band transition elements are not included on this plot.

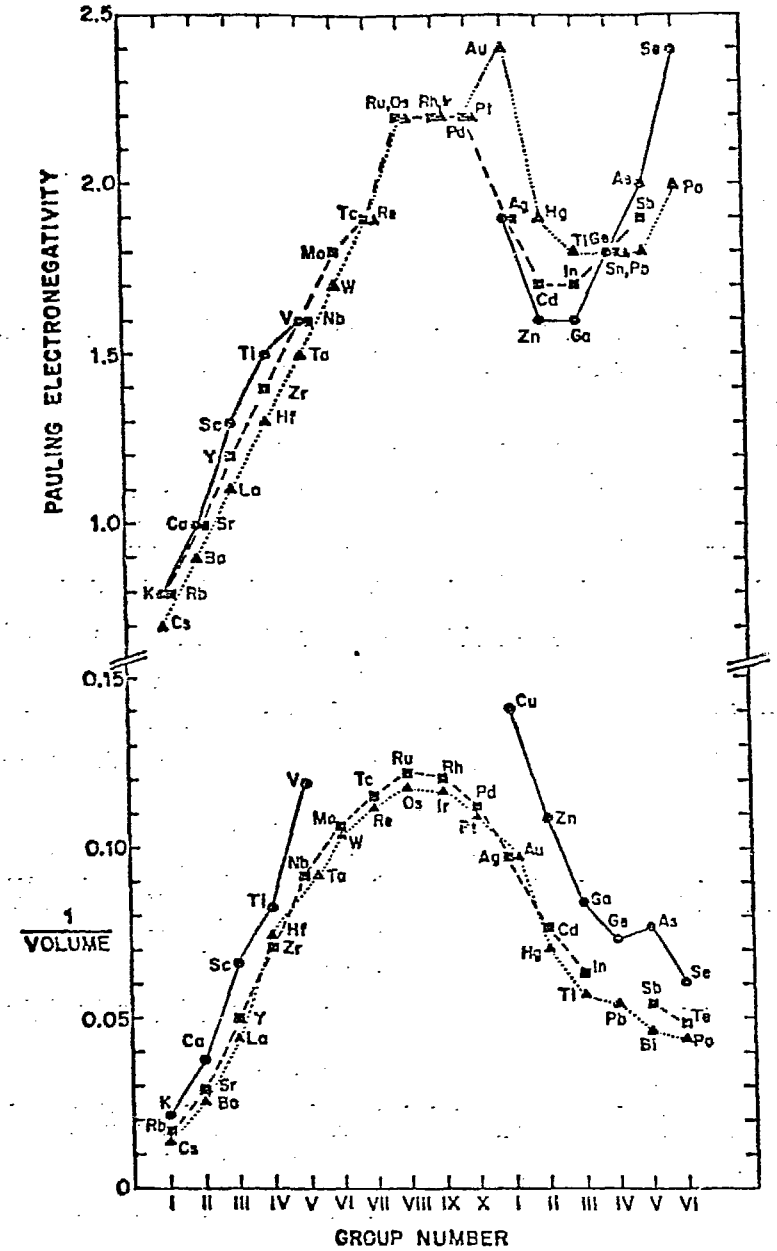

Fig. 2 - Pauling electronegativity (upper plot) and inverse volume (lower plot) against periodic chart group number, for the elements.

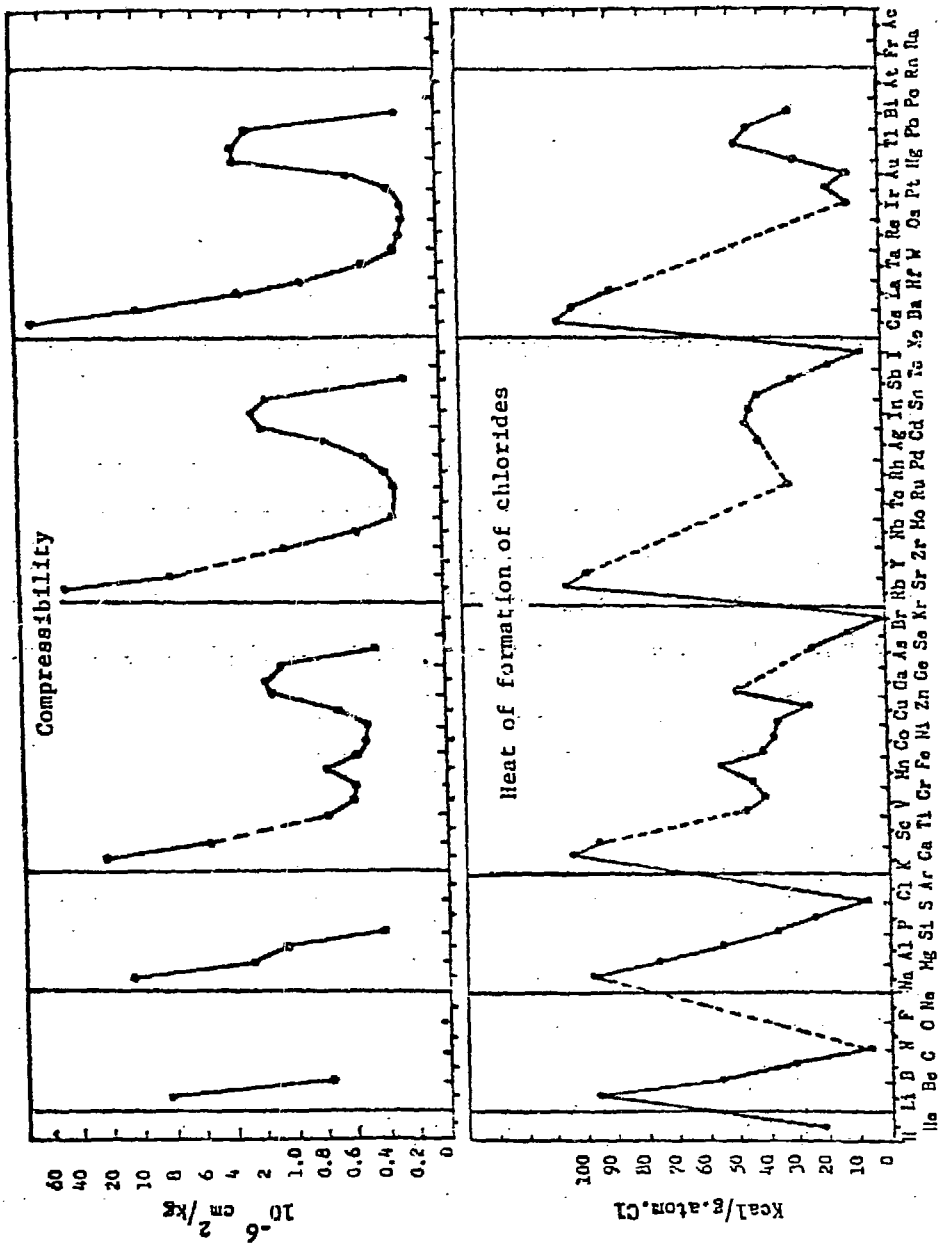

Fig. 3 - Two measured quantities (compressibility and heat of formation of chlorides) for the elements of the periodic table. [from Graphic Handbook of Chemistry and Metallurgy by P. Y. Loung (Chemical Publishing Co., Inc., 1965)].

where the r's are the atomic radii of the constituents A and B. C is a small constant which depends on the column(s) of the periodic table in which A and B reside. On other occasions, Pauling introduced a correction to bond length based on the number of valence electrons in the bond. In a review of the so-called geometric factor in catalysis, Ertl (8) recalled a hypothesis of Smoluchowski that the work-function of a stepped-surface will be lower than that of the plane surface, and thus the effect of surface geometry on catalysis cannot be considered independently from electronic effects. Closer to the problems at hand, the area associated with an atom's Wigner-Seitz cell surface enters a concentration dependent factor in Miedema's description of heats of formation. The areas of the constituents are adjusted to account for charge flow with a term $C'(\phi_A-\phi_B)$ where again C' depends on the position(s) of the elements in the periodic table. In addition to being interrelated, the basic physical parameters cannot, in general, be uniquely defined. Consider the different values of valence assigned to copper (Table I). For another parameter, ionic, covalent and metallic "sizes" have been used for the elements. Size may also depend on the coordination number, that is, the number of atoms immediately surrounding the atom in question: Geller, has introduced (9) a set of metallic radii appropriate to the A15 structure which includes such compounds as superconducting Nb_3Sn. These radii differ significantly from the "normal" metallic radii because of the peculiar packing in this structure. Pearson (3) has discussed the size-coordination number problem. The relation of volume to charge transfer has been considered elsewhere (10).

In deference to limited space, we will concentrate on one of the parameters, the electronegativity, in this review. The first part of this paper will deal with the various ways an electronegativity scale may be defined. Implicit in a given definition is some model of the bonding tendencies described by a set of electronegativity values. In the course of considering these matters, we will extend an earlier estimate (11) of a Mulliken electronegativity scale to include the transition elements. The Mulliken approach (12) involves free atom ionization energies and electron affinities, or in other words, an atom's tendency to keep its own valence electrons and compete for others. Coulson has argued (13) that this type of scale has, in its simplicity, a precise experimental and theoretical foundation. We agree with Coulson's view, at least for the non-transition elements. However, the transition elements are characterized by the large number of d-states near the Fermi level. The tendency for charge transfer in alloying transition elements depends not only on a single energy characterisitic of these states, but, importantly, on how many of these states are occupied, and how many are empty. This matter will be discussed here briefly; an approach incorporating such effects is considered in greater detail (14) in another chapter of these proceedings. Having considered the various choices of electronegativity scales we will also examing a suggestion (15,16) of Simons and Bloch for a second parameter, for main group elements, which is a measure of the relative tendency for the s versus the p valence electrons to be involved in bonding. Simons defined these factors in terms of effective orbital radii which, crudely speaking, are the inverse of

the ionization energies. There are subtle differences in electronegatvity and s-p bonding scales defined in terms of radii as against energies. These trends will be explored. Finally we will review the use of such parameters in structural maps where it will be seen that the structure in which a particular compound forms correlates strongly with the values of the parameters. The maps are quite successful in differentiating between structures without any explicit reference to the relative sizes of the constituents. Remember, however, that size and electronegativity are not unrelated. Maps will be considered for compounds between main group elements, between transition and main group elements and, finally, among transition elements. The latter example will involve the σ and structurally related phases. Although the systems were chosen because they are very much alike, considerable order is found on the structural map.

While this review concentrates on the electronegativity parameter and one metallurgical application of it, we hope the reader will keep in mind the larger view: the parameters we use to describe alloy and compound behavior are related to one another and are not uniquely defined. In his summary of the 1966 Battelle conference, Lomer called (17) for a multivariant analysis of the parameters used to describe alloys. Such techniques are commonly used by sociologists but perhaps our data base is too sparse and too unreliable. There have been real advances during the last decade in our understanding of alloys as can be seen by comparing these proceedings with those for the Battelle meeting. Despite this, Lomer's task remains undone.

II. Electronegativities

The idea of a parameter which summarizes the ability of one atom to compete with another for valence electron charge is central to much thinking concerning compound and alloy formation. Early on it was recognized that electronegativity cannot be described simply as a universal constant appropriate to each given element. Effective electronegativity scales have been seen to depend on the environment in which the element finds itself and on the atom's electronic configuration (6,18), e.g. do we have carbon in its covalent $2s2p^3$ or its more metallic $2s^22p^2$ configuration? The inability to define a unique scale is only partially due to the fact that the use of a particular set of experimental data or theoretical calculations may have implicit size, electron density and other contributions built in. Equally important, physical effects that we would like to describe in terms of an electronegativity trend, e.g. bond energies, are more complex than the simple matter of attracting charge. What is more, different valence electrons play differing roles in bonding. The main group elements have s and p valence electrons. While a monovalent element, such as Na, involves primarily s electrons, and polyvalent Sb primarily p, an interplay of s and p bonding is involved for all these elements. Similarly the transition elements have relatively localized d electrons and relatively diffuse s-p "conduction" electrons. Despite their localization, the d electrons are important to bonding because of the large number of states close to the Fermi level - what is important here is the different character

of d and non-d bonding effects (14). Valence electron bonding thus involves a subtle mixture of bonding, charge transfer and screening effects and we require an electronegativity scale which summarizes the gross effect plus recognition of more subtle factors and of when these subtle factors are of significance to alloy formation. Simons and Blochs' work (15), which will be described shortly, is an important effort of just this sort for the main group elements.

Electronegativity scales, ϕ, have been defined in a number of contexts as is indicated in Table II. The three most popular classes of scales are derived from ideas normally attributed to Mulliken (12), to Pauling (7) and to Gordy and Thomas (2,19). Mulliken suggested defining ϕ in terms of the average of the free atom valence electron ionization energy, ε, and the electron affinity a, i.e.

$$\phi = C\left(\frac{\varepsilon+a}{2}\right) \tag{2}$$

where C is a constant. By averaging the cost to lose, and the energy associated with gaining, valence electron charge one makes simple contact with the normal definitions of ϕ - namely the tendency to attract and hold valence charge. Although it involves effective radii, the St. John and Bloch electronegativity scale, which will be considered later in this section, may be said to be of the Mulliken class. Granted that the environment affects ϕ, it can be argued that one should define ϕ in terms of data appropriate to compounds rather than to free atoms. Pauling based (7) his ϕ on thermochemical data and, more recently, Phillips provided an alternate derivation (20) based on the dielectric properties of solids. Pauling's scale is based primarily on data for covalently, rather than metallically, bound systems and questions can be raised concerning modifications necessary for applications to metallic systems for such strongly covalent elements such as C, N and Si. We believe (11) that this is particularly important for transition metal carbide and nitride formation. The Gordy-Thomas scale is derived from the work functions of the pure elements in their solid state. The work function is a measure of the position of a solid's Fermi level and the Fermi level, by another name, is the chemical potential. Presumably the element with the higher lying Fermi level loses charge to the component whose level lies lower so that the two ε_F equilibrate[+]. The work function is not an entirely satisfactory measure of the chemical potential because it defines the Fermi level with respect to the external vacuum zero for a crystal with a surface dipole layer. One would prefer having the Fermi levels of the alloy constituents defined with respect to a common zero within a crystal. Despite any formal shortcomings, electronegativity scales based on work functions are used frequently,

[+]As is discussed elsewhere in these proceedings[14], we do not believe that the relative positions of local ε_F determine charge transfer in an alloy consisting of transition elements. Instead it depends on a transition metals' tendency to gain or lose d charge by hybridization of its partly filled set of d levels with the other alloy constituent.

TABLE II

ELECTRONEGATIVITIES

SPECTROSCOPIC - ATOMIC IONIZATION ENERGIES AND ELECTRON AFFINITIES

R. S. Mulliken, "A New Electroaffinity Scale; Together with Data on Valence States and on Valence Ionization Potentials and Electron Affinities", J. Chem. Phys. 2, 782 (1934).

R. S. Mulliken, "Electronic Structures of Molecules. XI. Electroaffinity, Molecular Orbitals and Dipole Moments", J. Chem. Phys. 3, 573 (1935).

R. S. Mulliken, Ref. 12.

H. A. Skinner and H. O. Pritchard, "The Measure of Electronegativity", Trans. Faraday Soc. 49, 1254 (1953).

J. Hinze and H. H. Jaffe, "Electronegativity, I. Orbital Electronegativities of Neutral Atoms", J. Amer. Chem. Soc. 84, 540 (1962).

J. Hinze, M. A. Whitehead and H. H. Jaffe, "Electronegativity. II. Bond and Orbital Electronegativities", J. Am. Chem. Soc. 85, 148 (1963).

J. St. John and A. N. Bloch, Ref. 16.

R. E. Watson and L. H. Bennett, Ref. 11.

EFFECTIVE CHARGE AND BOND RADIUS

W. Gordy, Ref. 2.

THERMOCHEMICAL

L. Pauling, "The Nature of the Chemical Bond. IV. The Energy of Single Bonds and the Relative Electronegativity of Atoms", J. Am. Chem. Soc. 54, 3570 (1932).

M. Haissinsky, "Echelle des Electronegativites de Pauling et Chaleurs de Formation des Composes Inorganiques, J. de Physique et Radium 7, 7 (1946).

M. L. Huggins, "Bond Energies and Polarities", J. Am. Chem. Soc. 75, 4123 (1953).

A. P. Altshuller, "The Electronegativities and Some Electron Affinities of Copper, Zinc, and Gallium Subgroup Elements", J. Chem. Phys. 22, 765 (1954).

L. Pauling, Ref. 7.

TABLE II - continued

SPECTROSCOPIC - DIELECTRIC PROPERTIES OF SOLIDS

J. C. Phillips, Ref. 20.

WORK FUNCTIONS

W. Gordy and W. J. O. Thomas, Ref. 19.

A. R. Miedema, F. R. deBoer and P. F. deChatel, "Empirical Description of the Role of Electronegativity in Alloy Formation", J. Phys. F 3, 1558 (1973).

A. R. Miedema and P. F. deChatel, Ref. 5.

HYPERFINE EFFECTS - DIPOLE, QUADRUPOLE, ISOMER SHIFTS

H. S. Gutowsky and C. J. Hoffman, "Nuclear Magnetic Shielding in Fluorine and Hydrogen Compounds", J. Chem. Phys. 19, 1259 (1951).

W. Gordy, "Interpretation of Nuclear Quadrupole Couplings in Molecules", J. Chem. Phys. 19, 792 (1951).

W. Gordy, "Relation of Nuclear Quadrupole Couplings to the Chemical Bond", J. Chem. Phys. 22, 1470 (1954).

R. E. Watson and L. H. Bennett, Ref. 22.

FORCE CONSTANTS

W. Gordy, "A Relation Between Bond Force Constants, Bond Orders, Bond Lengths, and the Electronegativities of the Bonded Atoms", J. Chem. Phys. 14, 305 (1946).

A. D. Walsh, "Factors Affecting Bond Strengths", Proc. Roy. Soc. (London) A207, 13 (1951).

A. L. Allred and E. G. Rochow, "A Scale of Electronegativity Based on Electrostatic Force", J. Inorg. Nucl. Chem. 5, 264 (1958).

GENERAL REVIEWS

H. O. Pritchard and H. A. Skinner, "The Concept of Electronegativity", Chem. Revs. 55, 745 (1955).

R. Ferreira, "Electronegativity and Chemical Bonding", Advan. Chem. Phys. 13, 55 (1967).

and with considerable success, for metallurgical problems. Recently Miedema rederived the scale for use in his model (5) of compound heats of formation. The extensive investigations of Darken-Gurry alloy solubility plots by the Los Alamos group (21) used the electronegativities of Gordy and Thomas which are based, in part, on charge screening considerations and, in part, on work functions. For the case of Au, the low value based on the work function was employed.

Three scales are plotted in Fig. 4. They have been brought to a common overall scale by linear regression of one set versus another. Work functions are represented by Miedema's values, the Pauling scale comes (6) from "The Nature of the Chemical Bond" and the Mulliken values are derived in the next section. Despite their diverse origins, the three scales are remarkably alike. There are, however, certain substantive disagreements. For example, the Pauling scale has Au the most electronegative of the metals while the Au work function ϕ is smaller than the ϕ of a number of transition metals to the left. The Pauling trend is consistent with Mössbauer isomer shift and photoemission results which suggest (14,22) that charge transfer is always off other metals and onto Au. On the other hand, Miedema's description of heats of formation requires that Au have a ϕ roughly equal to that of W. These metals have a positive heat of formation while elements to the left <u>and</u> right of W have negative heats of formation when alloyed with Au. This implies a small electronegativity difference, $\phi_{Au} - \phi_W$, and larger differences when the other elements replace W because it is a term involving the difference in ϕ which makes the negative contribution to a heat of formation in Miedema's scheme. In considering Au, and for that matter Ag and Cu as well, it would appear that different electronegativity trends, relative to the transition elements, are necessary in order to rationalize different experimental facts. Miedema has suggested that his <u>two</u> parameters, <u>taken together</u> provide a basis for describing charge transfer. In this sense Miedema's ϕ is expected to systematically differ from other ϕ scales. While alloying of transition and noble metals involves local chemical potential shifts, active d-band hybridization and non-d screening and bonding, the relative roles of these factors may differ between the two group of elements. This would imply that no single electronegativity parameter can summarize the bonding effects as seems to be the case.

A few years ago, Simons and Bloch developed (15) a pseudopotential approach to bonding among the main group elements. Now pseudopotentials aren't new. Perhaps the first pseudopotential approach to electronegativity is represented in Fig. 1 where the ordinate is an effective charge divided by a radius and hence is an effective potential. The valence, n, was taken to equal 1 for the noble metals and they are found to lie off the line (as do the more than half filled or antibonding d-band transition elements which aren't represented in the plot). Attributing a valence of 4 or 5 brings the noble metals onto the line. These large valences for the noble and adjacent transition metals which the solid-state physicist finds so odd are just what Pauling (7) proposed (see Table I).

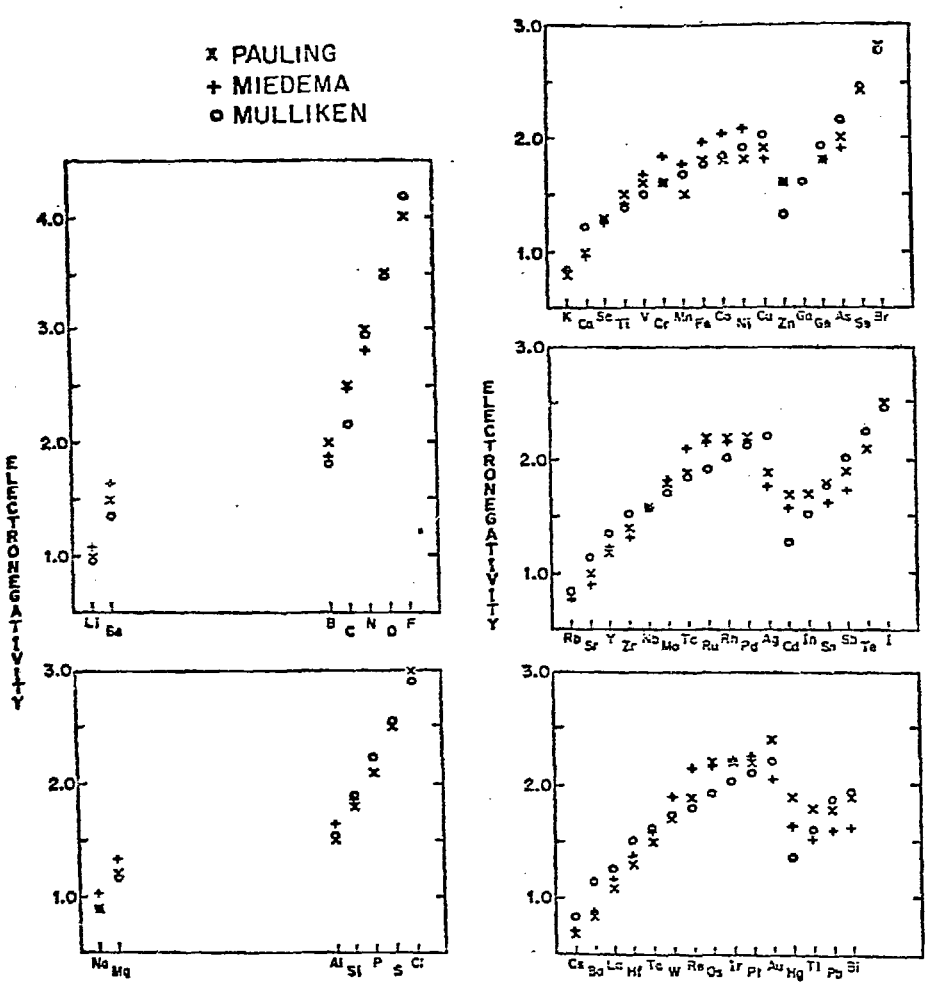

Fig. 4 – Comparison of three electronegativity scales, for elements of five rows of the periodic table. Note that both the Miedema and the Mulliken scales have been modified for this comparison by linear regression to the Pauling (6) scale. The Mulliken scale is derived in the text, Section III.

Pseudopotentials have evolved considerably since 1946. In particular, the implications of employing non-local pseudopotentials have been explored. One of the simplest nonlocal pseudopotentials is one where electron orbitals of different angular quantum number ℓ see different potentials. Chelikowsky and Cohen have shown (23) that it is necessary to employ ℓ dependent pseudopotentials in order to calculate the correct shape of the bonding charge in semiconductors. Simons' approach also involves ℓ dependent potentials. He introduced an effective orbital quantum number $\hat{\ell}$, defined in terms of the experimental binding energy, $\varepsilon_{n\ell}$, for a single valence electrons outside an ion core,

$$\varepsilon_{n\ell} = \frac{-Z^2}{2[\hat{\ell} + 1]^2} \tag{3}$$

For those familiar with quantum defect theory, the quantum defect has been introduced into ℓ rather than into Z, which here is the charge of the ion stripped of its valence electrons. The resulting $\hat{\ell}$ introduces an $\hat{\ell}\,(\hat{\ell}+1)/r^2$ term in an effective potential for the electron and also defines an effective orbital radius

$$r_\ell = \frac{\hat{\ell}(\hat{\ell} + 1)}{Z} \quad . \tag{4}$$

Simons and Bloch suggested that the difference

$$S \equiv r_p - r_s \tag{5}$$

for the valence s and p electron provides a measure of the relative tendency for the s versus the p electrons to be involved in bonding. More will be said of this in Section IV. St. John and Bloch defined (16) an electronegativity scale in terms of these radii with

$$\phi = a\,[1/r_p + 1/r_s] + b \tag{6}$$

where a and b were obtained by fitting the ϕ of the 2s-2p elements to the Pauling scale. More recently it has been shown (24) that the r_ℓ of Eq. 4 are not true measures of valence orbital size (in fact they lie inside the radii of the ion cores of the heavy polyvalent elements). This does not matter because they display a one-to-one mapping onto the true orbital radii as obtained, say, from the expectation values of $\langle r^{-1}\rangle$ for free atom Hartree-Fock orbitals.

Inspection of Equations 3 and 4 indicates the $1/r_\ell$ varies roughly as $\varepsilon_{n\ell}$ suggesting that Mulliken and the St. John and Bloch scales are roughly equivalent if St. John and Blochs' $\varepsilon_{n\ell}$ were inserted into Eq. 2. There are subtle, systematic valence dependent differences between a scale employing radii and one employing ionization energies as can be expected from the trend illustrated in Fig. 5. The ε are experimental s and p ionization energies of the neutral atoms and $(1/\langle r_s\rangle + 1/\langle r_p\rangle)$ involves neutral atom Hartree-Fock $\langle r^{+1}\rangle$ values.

III. A Mulliken Electronegativity Scale

Previously we defined (11) a Mulliken electronegativity scale for the main group elements in terms of the neutral atom s and p electron ionization energies. The electron affinities, a, of Eq. 2 were omitted because few are known experimentally. Those that are known, indicate a ratio $a/\varepsilon \sim 0.1$. In other words the values of a are small, scale roughly with ε and, if the constant C is scaled accordingly, their omission has at most a few percent effect on the resulting ϕ. The ε were obtained by using neutral atom spectroscopic data and taking averages over the multiplet levels of any given atomic configuration. A treatment employing only s and p terms is not applicable to the transition elements: not surprisingly, the transition elements have ϕ characteristic of the alkali earths on such a scale. We have obtained the average of configuration values of ε_s, ε_p and ε_d for the transition and noble metals. We can then define

$$\phi \equiv A\,\varepsilon_s + B\varepsilon_p + C\varepsilon_d + D \qquad (7)$$

where, for the main group elements, ε_d is set equal to the ionization energy of the first unoccupied valence d level. [The ε_d for the main group elements are small and, with one exception, almost constant. The main group ε_d therefore have a modest role in affecting the ϕ values of the main group elements relative to the transition elements but little effect on the ϕ within the main group elements themselves. The exception occurs for Ca, Sr and Ba which sit just below the onset of the 3d, 4d and 5d series. The unoccupied valence d levels lie abnormally low in energy, causing abnormal amounts of d character to be present in the occupied electron bands of these alkali earths. Their ε_d are intermediate between values characteristic of the main group and the values appropriate to Sc, Y, La or Lu which mark the start of the three transition series. One expects that it is appropriate to include this tendency in a Mulliken scale.] A, B, C and D are constants which have been chosen, subject to being kept positive, so that the resulting ϕ best match the Pauling scale yielding

$$\phi = 1.883\,\varepsilon_s + 1.463\,\varepsilon_p + 2.670\,\varepsilon_d + 0.249\,. \qquad (7a)$$

Since ε_p is almost proportional to ε_s, changes in the relative weight of the s and p terms have little effect on the ϕ values of the main group elements. The relative weight of d versus s plus p is essential to the placement of the transition and noble metals versus the main group.

The values appropriate to Eq. 7a are shown in Fig. 4. The ϕ for the main group elements have changed only slightly from the previously published values [A three to one p to s weight was used in the analogue of Eq. 7 previously. As noted, the change in s versus p weight has little effect on the results.] As was noted before, the Mulliken values for divalent Zn, Cd and Hg lie markedly lower than they do on the other two scales. On the other hand, with their atomic d shells more tightly bound, Cu, Ag and Au have larger ϕ than the transition elements residing in the same rows of the periodic table. Better overall agreement would be obtained

between the Mulliken and the other two scales if the ε_d term were turned partly off for the noble metals and if it were left slightly on for Zn, Cd and Hg. The d shells of Zn, Cd and Hg are sufficiently tightly bound core levels that one is hard pressed to justify their inclusion in Eq. 7.

The shortcoming of the Mulliken approach is that, while energies are dealt with, no account is made of the relative numbers of occupied and hole levels available for bonding. For the transitions and noble metals, in particular, there are a large number of occupied and hole states close to the Fermi level and it is the competition between the interatomic hybridization of these two groups of states which is essential to their bonding. This is discussed elsewhere in these proceedings.

The St. John and Bloch and the Mulliken scales are plotted versus the Pauling ϕ for the main group elements in Figs. 6 and 7 respectively. Except for the mismatch associated with the divalent elements, the Pauling and Mulliken scales map quite well against one another. Almost as good is the agreement for the St. John and Bloch scale, however, there are distinct lines, each associated with a particular valence. The trends are almost identical to those seen in Fig. 5. It would appear that there are subtle differences in scales employing radii and energies and these differences are nearly independent of how the radii were obtained. Here we have two nominally independent scales, size and energy, which show almost perfect correlation.

IV. Orbital Effects and Structural Maps

The principle purpose of the ℓ-dependent pseudopotential investigations of Simons and Bloch was to provide some measure of the relative role of s versus p electron bonding among the main group elements. The result was the S factor of Eq. 5. St. John and Bloch employed (16) this in the structural map shown in Fig. 8. One coordinate is the difference in electronegativities of the elements involved, the other is the sum of the S factors. The plot is concerned with the so called octet compounds where there are eight valence electrons per 50-50 molecule and the point of the plot is that different structures occur for compounds falling in different regions of the plot. The correlation of the various structures with electronegativity difference has been recognized for some time. Given the two parameters together, the structures fall into well defined regions: for example the rock salt and wurtzite structures are resolved though neither $\Delta\phi$ nor (S_A+S_B) alone suffices - Machlin, Chow and Phillips extended (25) the analysis to those nonoctet AB compounds having fewer than eight valence electrons per formula unit.

The experience of the preceding section suggests that ionization energies may replace radii yielding

$$S = (r_p - r_s) \propto \left(\frac{1}{\varepsilon_p} - \frac{1}{\varepsilon_s}\right) = \frac{\varepsilon_s - \varepsilon_p}{\varepsilon_s\,\varepsilon_p} \rightarrow (\varepsilon_s - \varepsilon_p). \qquad (8)$$

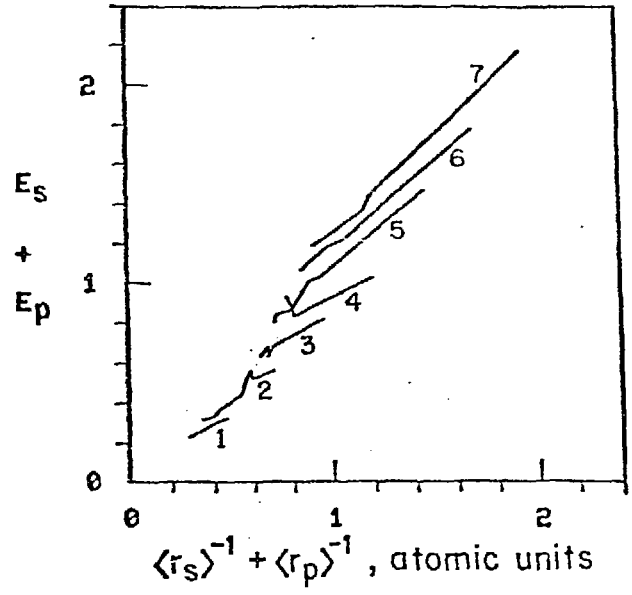

Fig. 5 - Sum of the experimental s and p ionization energies, in Hartree units (∿ 27eV) versus the sum of the inverses of the s and p orbital radii expectation values, obtained from neutral atom Hartree-Fock calculations for main group elements. The numbers 1-7 are columns of the periodic table ("group numbers"). Group 1 represents the alkali metals, group 2 the alkaline earths and Zn, Cd, Hg and so on. Note the systematic dependence on valence, evidenced by the near parallel lines, superposed on an almost linear correlation.

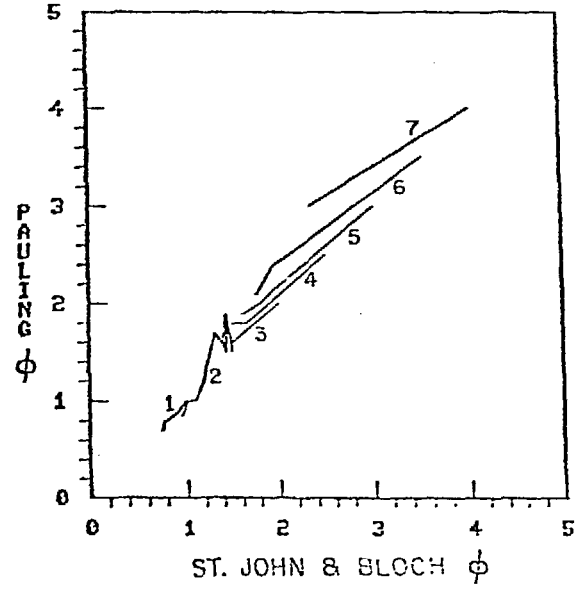

Fig. 6 - A plot of the Pauling (7) versus the St. John and Bloch (16) electronegativities for the same nontransition elements of Fig. 5. Note the systematic valence dependence here, as well.

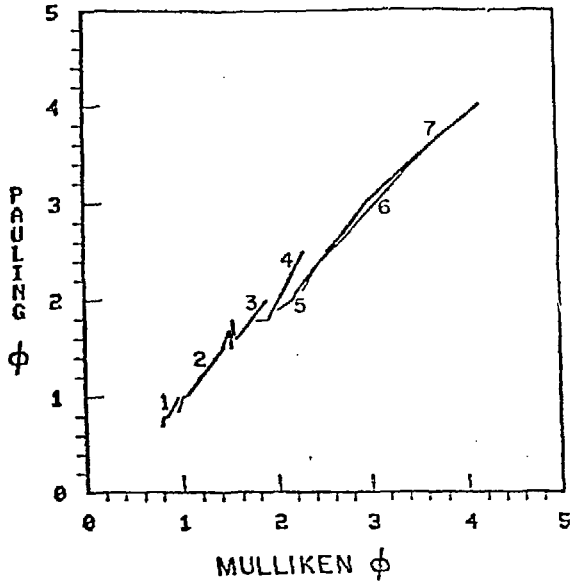

Fig. 7 – A plot of the Pauling (7) versus the Mulliken (12) electronegativities for the same elements as Figs. 5 and 6. Note the lack of valence dependence, except for group 4 (C, Si, Ge, Sn, Pb).

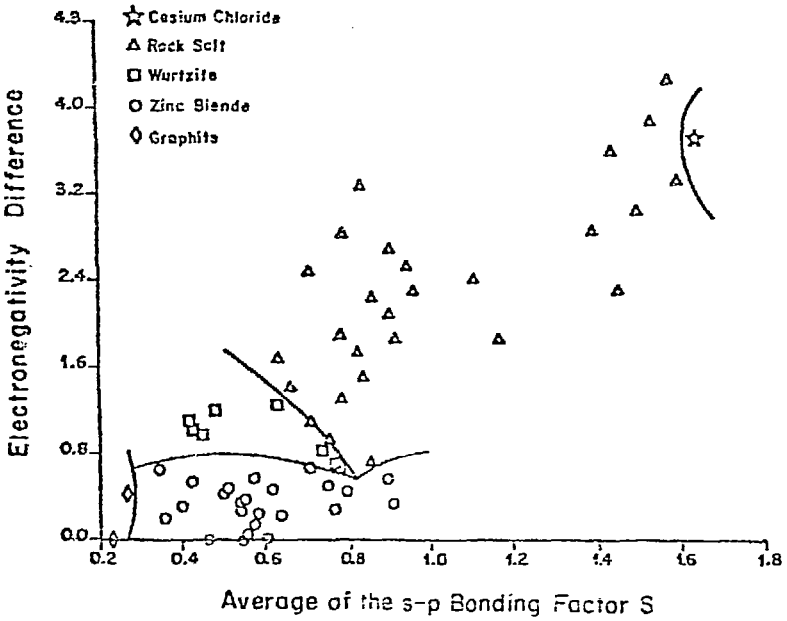

Fig. 8 – St. John and Bloch (16) electronegativity differences, $[(r_s(A) + r_p(A)) - (r_s(B) + r_p(B))]$ for $A^N B^{S-N}$ nontransition metal binary compounds versus the average of the s-p bonding factor S, $[((r_p(A) - r_s(A)) + (r_p(B) - r_s(B))]$. The s and p radii are defined in Eq. 4.

We have found it convenient (11) to employ the unnormalized form, as given in the second line of the equation. We applied this to a structural map of the nonoctet AB compounds with similar success to that of Machlin et al. In particular, the NaTl and CsCl structures fall into well defined regions with a mapping which makes no explicit reference to atom size and packing considerations.

The Mulliken electronegativities of Fig. 4 have been used in the structural map for main group AB_2 compounds shown in Fig. 9. Hydrides, oxides and halides are omitted from the map. The *sign* of the electronegativity difference is defined

$$\Delta\phi \equiv \phi \text{ (minority element)} - \phi \text{ (majority element)}. \qquad (9)$$

The weighted average

$$\frac{S_A + 2S_B}{3}$$

is used for the other coordinate. Except for $CaAl_2$ (having the $MgCu_2$ structure) and KPb_2 (the $MgZn_2$ structure), the structures fall in well defined regions on the plot. The boundaries have been drawn to guide the eye and have no theoretical significance. Both AB_2 and AB_3 compounds are represented on Fig. 10. There are more compounds out of position, but other than the AlB_2 and Ni_3Sn structures which tend to exist in the same region, different structures fall in reasonably well defined different regions of the plot. Three compounds forming in both the Cu_3P and Bi_3F structures are seen to fall on the natural boundary between the two structures. The success of the plot relies on *both* the S and the $\Delta\phi$ coordinates and on differentiating as to whether the majority or the minority element is the most electronegative.

A similar degree of success is obtainable for compound formation between main group and transition elements. Fig. 11 shows a map (11) for AM_2 compounds where the transition metal is the major component. The S factor of the A element *alone* has been used as one component. While the boundaries are not well defined, rather few compounds lie far outside the region of like structures. The $PbCl_2$ structure is unusual in that the structure occupies two distinct regions: one where the A site is more electronegative and another where it is more electropositive. The same thing would have occurred for the $PbCl_2$ structure in Figs. 9 and 10 if the halides had been represented in the plot. Otherwise, unless a near zero value of $\Delta\phi$ occurs, structures tend to be associated with a single sign of $\Delta\phi$. Related structures are found to lie adjacent to one another and to occasionally comingle. The three Laves' structures, C14 ($MgZn_2$), C15($MgCu_2$) and C36($MgNi_2$) provide an example of this in Fig. 11 as do the C23($PbCl_2$) and $B8_2$(Ni_2In) pair.

Although the abscissas of Figs. 9 and 11 are differently defined, there are some common features to the non-transition elements plot AB_2 and the non-transition-transition plot AM_2. If it

TABLE XII

$PbCl_2$	$MgZn_2$	CaF_2	$MgCu_2$	AlB_2	CaC_2 [a]	Cu_3P	Na_3As	BiF_3 & other [b]	BiF_3	Ni_3Sn	$AuCu_3$
Ca_2Ge	$MgZn_2$	BBe_2	$CaBi_2$	AlB_2	CaC_2	AsK_3	$AsRb_3$	Bi_3K	$InSr_3$	$LiHg_3$	Bi_3Sr
Ca_2Pb	$BaMg_2$	CBe_2	KBi_2	$SrGa_2$	BaC_2	$AsLi_3$	K_2NaSb	Bi_3Rb	$BiCs_3$	$CaHg_3$	Ca_3Pb
Ca_2Si	$CaCd_2$	$LiAlSi$	$RbBi_2$	$AlCaSi$	SrC_2	$AsNa_3$	K_3P	Li_3Sb	$BiLi_3$	Cd_3Mg	$CaPb_3$
Ca_2Sn	$CaLi_2$	K_2S	$CaAl_2$	$BaGa_2$	MgC_2	$BiNa_3$	Rb_3Sb		Ca_3In	$CdMg_3$	$CaSn_3$
	$CaMg_2$	K_2Se		$BaSi_2$		K_3Sb			Li_3Hg	$SrHg_3$	$CaTl_3$
	KNa_2	$KeTe$		$CaGa_2$		Li_3P			Li_2MgPb	$SrIn_3$	$NaPb_3$
	KPb_2	Li_2S		$NaHg_2$		Na_3P			Li_3Pb		$InCd_3$
	Mg_2Sr	Li_2Se		MgB_2		Na_3Sb			Ca_3Tl		$PbTl_3$
		Li_2Te		$CaHg_2$					$CdGeLi_2$		
		Mg_2Si							$CdSnLi_2$		
		Mg_2Ge									
		Mg_2Sn									
		Rb_2S									
		Na_2Te									
		Na_2Se									
		Na_2S									
		NaZnAs									
		LiZnAs									
		LiZnP									
		LiMgSb									
		LiMgP									
		LiMgPb									

a. CaF_2 and closely related MgAgAs structures

b. BiF_3 and another structure (either Cu_3P or Na_3As)

were assumed that the transition elements, M, make a contribution to S such that the AM_2 alloys take on an $\bar{S}$ value of about half the S_A of Fig. 11, the C_1, C_{14} and C_{23} compounds of the two figures would lie in the same regions. The only other common structure C15 is seen to lie to the right of C14 in Fig. 9 and the left in Fig. 11. This is related to the well-known characteristic of the Laves phase diagrams. For alloys involving only transition elements, there are regions of C15 stability to either side of C14. The structural map to be discussed in Section VII displays this also.

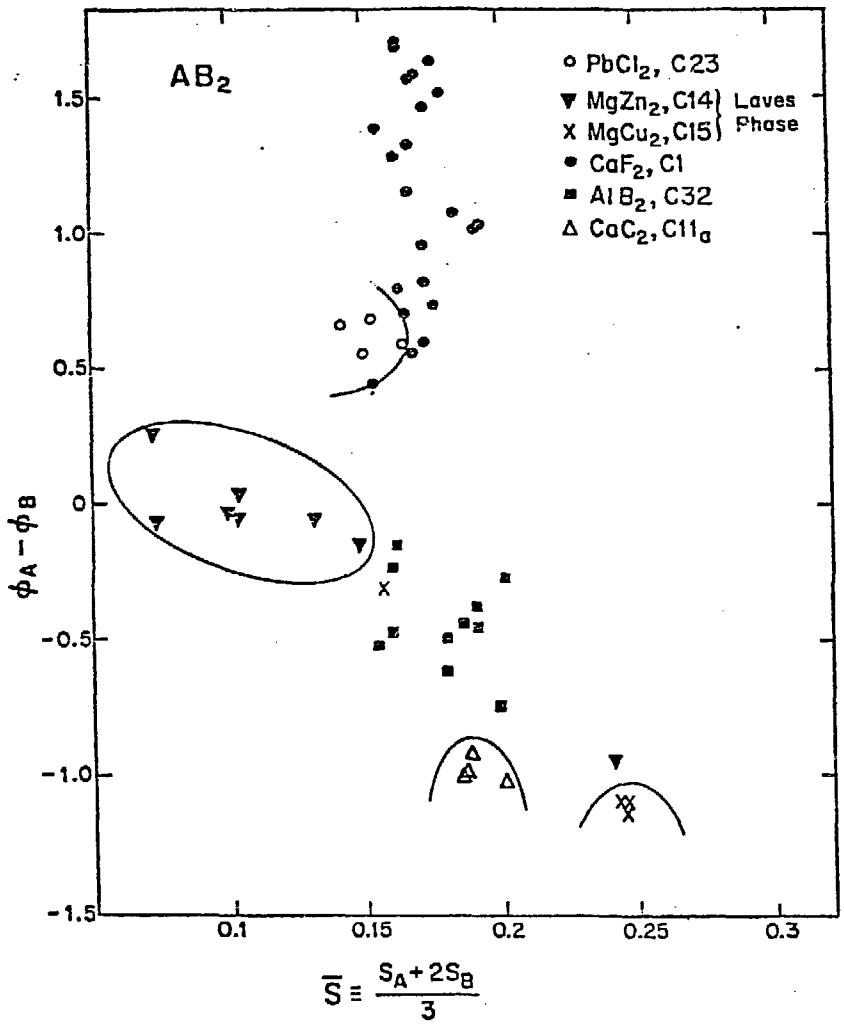

Fig. 9 - The structures of AB_2 compounds, formed from non-transition elements A and B, as a function of the Mulliken electronegativity difference and of the average S factor. The compounds plotted are listed in Table 3.

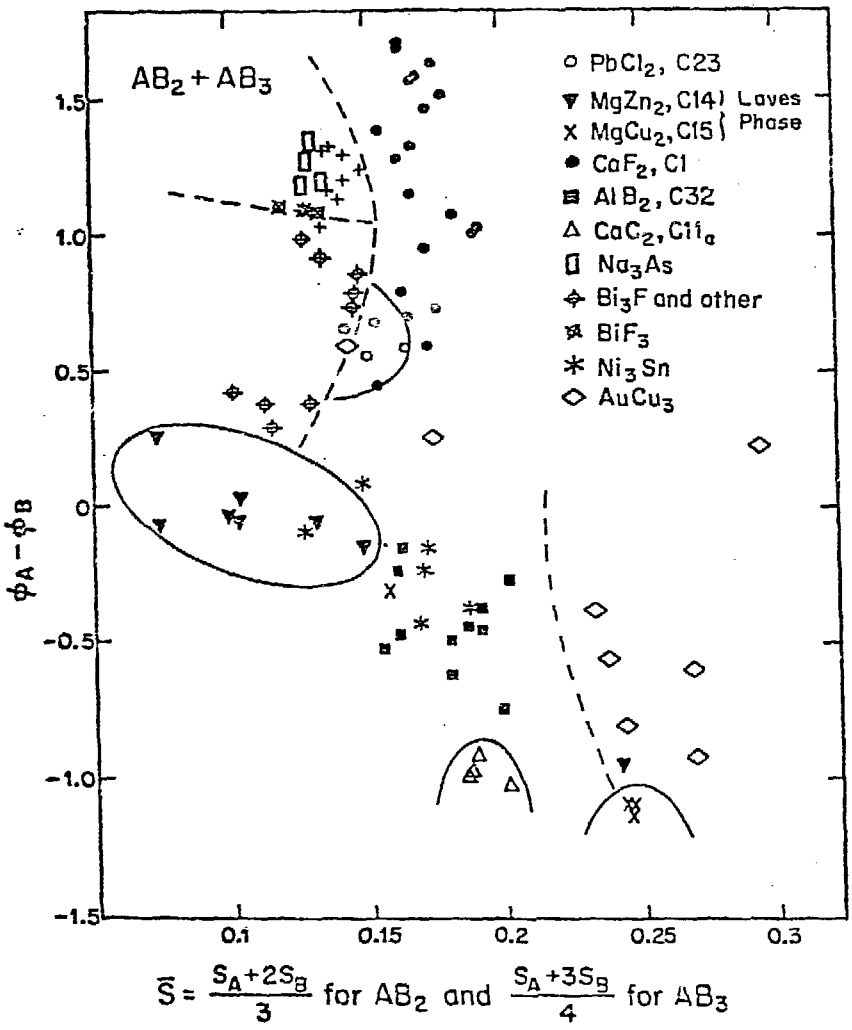

Fig. 10 – A composite plot of AB_2 compounds (from Fig. 9) and AB_3 compounds. The ordinate is the difference of the Mulliken electronegativies of Fig. 4. The abscissa is the average S factor. The compounds plotted are listed in Table 3.

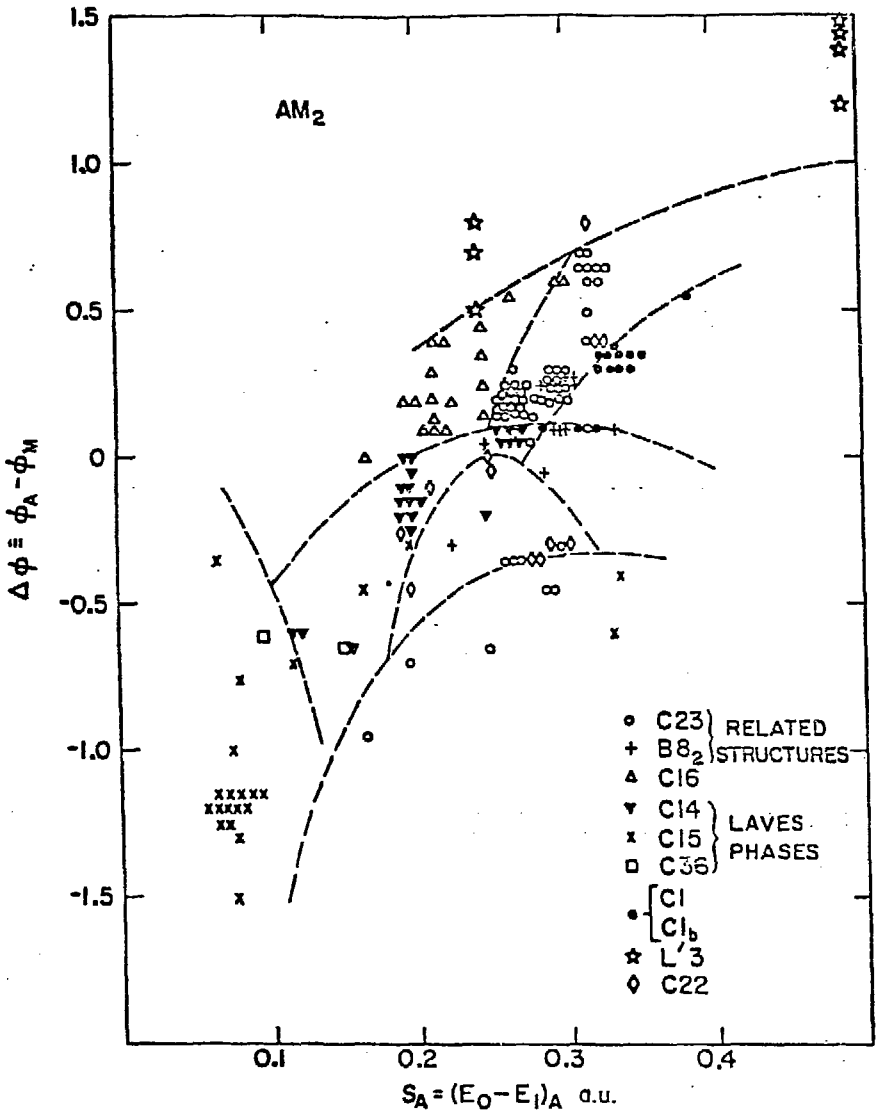

Fig. 11 - The structures of AM_2 compounds (A is a main group element, M a transition element) as a function of electronegativity difference and the A atom S factor. The compounds plotted are listed in Ref. 11.

V. Promotion Energy Effects

The s-p bonding factor defined in Eq. 8 is a promotion energy though, for polyvalent elements[+], its definition, the difference in ionization energies of the two shells, is somewhat different than the traditional definition (7)

$$E\ (\text{promotion}) = E(s^{n-1}p^{m+1}) - E(s^n p^m), \qquad (10)$$

which is the energy to promote one electron out of the valence s and into the valence p shell in the neutral atom.

In introducing their radius based S factor, Simons and Bloch were endeavoring to define a second electron factor to complement the electronegativity term. Being a "second" factor to complement presume that its effects are subtle and small - that it may be important to the structure of a compound but not to its heat of formation. As soon as S is identified as being a promotion energy there is the implication that it is of energetic significance. The familiar promotion energy of carbon, promoting the $2s^2 2p^2$ ground state to the tetrahedral bonding $2s2p^3$ configurations is 97 kcal/gm at.

There is unfortunately little experimental information concerning s-p promotion effects among main group elements in metallic compounds. The Mossbauer isomer shift (27) provides a measure of valence s electron count. Of the main group Sn and Sb (and to a lesser extent Te and Zn) have nuclear transitions suitable for such measurements. Sham et al. (28) have inspected the sequence AuSn, $AuSb_2$ and $AuTe_2$, using the isomer shift to infer the main group valence s change, Δn_s, and photoemission to indicate the net charge change, δ, where

$$\delta = \Delta n_s + \Delta n_p \ . \qquad (11)$$

In all three cases δ was found to be negative, i.e. charge was lost to A. . However Δn_s was roughly equal to δ for Sn, smaller but the same sign for Sb and probably of reversed sign for Te, i.e. Te s count increased while net valence charge was lost. The uncertainties in the analysis are considerable but it would appear that, in addition to net charge transfer, there is change in the relative s to p count which varies by $\sim$ 0.1e across this set of compounds. Now, the promotion energies of Sn, Sb and Te are expected to be larger than that of C and the implication of a varying promotion (or demotion) energy of $\sim$ 0.1e is a term which varies by roughly 10 kcal/gm at. across this sequence of compounds. This is to be

[+]In the case of the mono and divalent elements, ε_s is defined for the ground atomic configuration which has only occupied s valence electrons. The ε_p are defined in terms of excited monovalent p' and divalent $s'p'^p$ configurations, i.e. ε_s is defined for an $s^n p^m$ and the ε_p for an $s^{m-1}p^{m+1}$ state in the sense of Eq. 10. In these cases Eq. 8 and 10 are identical and S is the traditional s-p promotion energy.

compared with the experimental heats of formation which (29) are -3 kcal/gm at. for $AuSn_2$ and -1 kcal/gm at. for $AuSb_2$ (we have found no value for $AuTe_2$ but would assume it's between 0 and -1 kcal/gm at.).

It is interesting to ask where such a term might reside in Miedema's scheme for alloy heats of formation. He has

$$\Delta H = f(c)\ [-P(\Delta\phi)^2 + Q(\Delta n^{1/3})^2 - R] \qquad (12)$$

where f(c) is a concentration dependent term; $-P(\Delta\phi)^2$ a negative term associated with differences in electronegativity; $+Q(\Delta n^{1/3})$ a positive term associated with the energy cost due to any mismatch in electron charge density at the surface of the atomic cells and -R is a "d-p bonding" term arising for compound formation between transition (or noble) and polyvalent elements. The value of R depends on whether a transition or noble element is involved and on what the valence of the main group element is. While the promotion effects might be buried in one of the first two terms of the bracket, we believe, in fact, that it is incorporated in the R factor. This matter requires further investigation.

VI. The Sign of the Electronegativity Difference Substitutional Alloying in the Fe_3Si System

Perhaps the most striking aspect of the structural maps of Figs. 9, 10 and 11 is the fact that the sign of the electronegativity difference, i.e. whether the majority or minority component is more electronegative, is important to the structure a compound takes. Recently Burch et al. have encountered (30) a similar trend when considering substitutional alloying effects in the Fe_3Si system. The Fe_3Si structure is shown in Fig. 12. One third of the Fe's are on B sites with eight Fe nearest neighbors, while the remaining two thirds are on A sites with four Fe and four Si nearest neighbors. Fe_3Si is magnetic, the B site Fe's have magnetic moments of 2.2 μ_B while the A site atom have moments of 1.4 μ_B and are believed to be somewhat more negatively charged (i.e. have excess electrons) than the B sites. Such a charge trend is expected if one assumes* Si to be more electropositive than Fe. Burch et al. were using nuclear magnetic resonance to study the effect of substitutional alloying. One byproduct of this was that they could determine what site an impurity went into. Some transitional impurities went into FeB sites, some into A sites and some could not be substituted. The results are summarized in Fig. 13. Impurities which are more electronegative than Fe go into the more negative A site while those which are less electro-

*This depends on what electronegativity scale one takes seriously. However, the Fe_3Al system displays similar behavior and it is generally agreed that Al is more electropositive than Fe. Part of the problem associated with Fe and Si may be that the ϕ values for Si are derived for the case of covalent bonding and here we are involved with more metallic bonding.

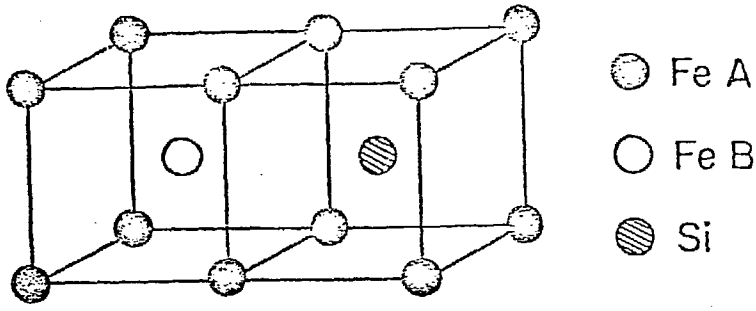

Fig. 12 - The Fe_3Si structure, differentiating between the two types of Fe site.

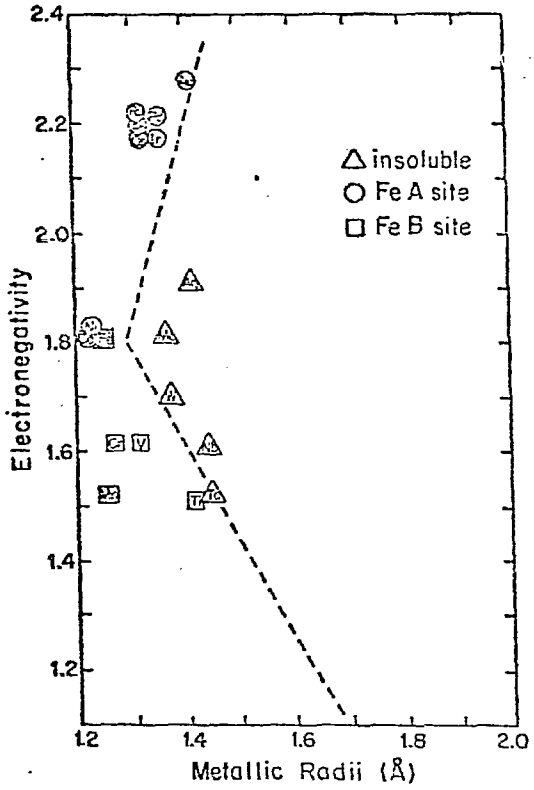

Fig. 13 - Substitutional alloying results in Fe_3Si (after Ref. 30). The more electronegative elements substituted for Fe on the A sites, the less electronegative elements for Fe on the B sites.

negative, namely Cr, Mn and V, go into the more positive E sites. Size mismatch inhibits substitution however, and increase in electronegativity difference improves the ability of an oversized impurity to be accommodated. This is the exact opposite to the experience of Darken-Gurry plots (see Gschneidner (4) in these proceedings) where alloy solubility occurs within some ellipse defined by

$$A(\Delta\phi)^2 + B(\Delta V^2)$$

where ΔV is the difference in the atomic volume of host and impurity and A and B are positive constants. Roughly speaking, B appears to have flipped sign in Fig. 13. Not altogether surprisingly, here is an example indicating that the roles of size and electronegativity can be quite different for substitutional solubility in compounds than they are for substitution in the pure elements.

Of more immediate concern to the subject of this paper is the physically appealing trend concerning the site preference of impurities depending on the sign of their electronegativity difference, relative to that of iron.

VII. Structural Mapping for Alloys of Transition Elements The Sigma and Structurally Related Phases

Application of structural maps to alloys between transition or noble elements require either an extension of the definition of S, the s-p promotion factor or its replacement by a different d-band parameter. Transition metal alloying involves (14) d bonding and its associated charge transfer, conduction electron screening of the d charge transfer and conduction electron bonding. Important to this are such factors as the relative availability of d band occupied levels and holes and such effects are not readily encorporated in a d-non d equivalent of Eqs. 5 or 8. One electron factor has proven of use in other correlations of metal properties, namely the electron vacancy or average number of holes per atom, h/a, in the d bands of the alloy. We have used d-electron vacancies for structural maps of NM, NM_2 and NM_3 (31) and for a map (32) of the σ and structurally related phases.

The sigma phase, a complex structure occurring in many transition metal systems, is of considerable practical and theoretical interest. Its presence can cause a normally ductile high performance steel or superalloy to embrittle and fail in service. There are a number of structurally related phases (33,34), some of which have properties which are of interest for other reasons. For example, the A15 structure includes the highest transition temperature superconductors, such as Nb_3Sn, while the $CaCu_5$ structure includes $LaNi_5$ which is an excellent hydrogen storage alloy, and $SmCo_5$ which is an extremely useful hard magnet. The stability of the σ phase has generally been discussed in terms of electron and size factors (35-37) in combination. The composition range of some σ phases is wide while in others it is narrow and the relative size of the constituent atoms, hence the ability of an atom to be at a "wrong" site, appears important to these trends (37). The fact that two transition metals are almost always involved in a σ phase alloy suggests that d-electron bonding is a dominant factor de-

termining phase stability. Electron effects are often incorporated in terms of a single factor, such as the hole count h/a. The σ phase typically occurs for an h/a 3 to 4 and compounds, forming in one of the structurally related phases have h/a values in this range. What is more, a significant fraction of the σ phase alloys form in another structurally related phase at some different composition and, experimentally, this is as likely to occur for a σ phase alloy with the "ideal" h/a ratio as for one without. Size does not appear explicitly in a map employing h/a and the electronegativity difference but, as has been seen earlier in this chapter, size is not unrelated to electron factors.

There is some degree of arbitrariness in constructing a list of structures related to the σ phase. We have taken these to include the Cr_3Si, αMn, μFe_7W_6, and the two Laves phases Cu_2Mg and $MgZn_2$. All appear in the Shoemakers' tabulation (33) of σ related structures. Their tabulation includes other phases not represented here because few or no binary transition metal alloys form in them. We have added $CaCu_5$ to the list because, as Nevitt (34) emphasizes, it is a structural variant of the Laves phases. There is considerable uncertainty in ascertaining which alloy systems form in which structures. When sources disagree, we have generally used the assignments in Landolt-Börnstein (26). The list of systems so chosen, and represented on the map are listed elsewhere (32). The electronegativity difference and the average d-band vacancy have in general been evaluated for the center of the composition range over which an alloy system occurs*.

The structural map appears in Fig. 14. The seven represented phases are indicated by separate symbols. In addition, there are a large number of cases in which a pair of elements are found take on two of the structures at two different compositions. Special symbols are used to denote the four most important cases where a phase is represented, but also occurs at another structure at some other composition. As with the earlier maps, the map is divided into regions associated with different structures and, the boundaries have been drawn to guide the eye and have no theoretical significance. As a general rule, points representing compounds again fall inside of, or lie close to, the appropriate structural region. The division of the map into regions involves a combination of the coordinates. A single electron factor alone is not sufficient to resolve the structures.

---

*The case of several of the μ phase compounds is an exception. The sign of Δφ was chosen on the basis of the prototype Fe_7W_6, where the element residing on the minority W site is taken to be the minority constituent, rather than on the reported stoichiometries. The A15 compound MoTc was also assigned on this basis. [Eq. 7 is undefined for the few alloys where this average is at fifty percent. Δφ was taken as positive in such cases.]

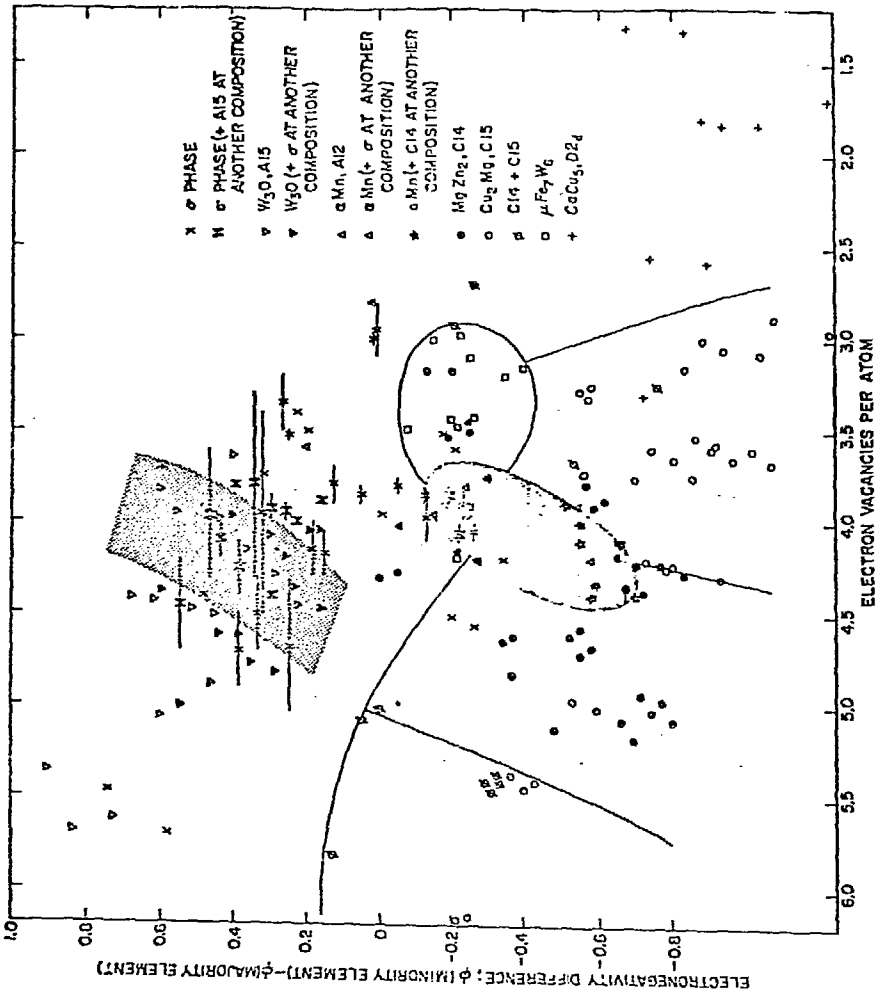

Fig. 14 – Map of the σ and structurally related binary transition metal alloy phases. The ordinate is the band theory electronegativity differences. The abscissa is the average d-electron vacancy count. The horizontal bars show stoichiometry ranges.

All regions lie either to one side or the other of the zero of $\Delta\phi$ with the exception of the σ phase itself which lies astride the zero. Unlike the other phases, some σ structure compounds display wide stoichiometry ranges (as indicated by the horizontal lines on the map) and different compounds form in the σ phase at markedly different stoichometry, e.g. CrFe and $CrMn_3$. Ranges of stoichometry are often associated with small $\Delta\phi$ and favorable size considerations and it is tempting to associate the wide variation in composition to the fact that the σ region lies across the zero--but note that the widest σ composition ranges occur for some of the largest $\Delta\phi$ values.

The two hatched areas of the map are regions of coexistence. The ellipse is associated with the αMn structure and overlaps the regions of the σ phase and the Laves structures. Over half the systems forming in the αMn phase also form in one of these two other structures. Those pairs of elements with near zero $\Delta\phi$, i.e., lying near to the σ region, tends to form in the σ structure while most of αMn systems with $\Delta\phi<-0.5$ form in the C14 structure instead. Many alloy systems form in both the σ and the A15 phases and the upper crosshatched region is the "boundary" where both occur. As a general rule the σ phase occurs with lower vacancy count than its A15 counterpart, hence a clustering of σ phases immediately to the right, and A15 phases to the left of the boundary region. The map thus displays orderliness in the coexistence of phases in alloy systems as well as in the existence of single phases alone.

It is interesting that there is a C15 region lying to either side of the C14. In the AB_2 and AM_2 maps of Figs. 9 and 11, the tendency for C15 to lie on opposite sides of the C14 was noted. It might then appear that there is a close relationship between the s-p parameter (S) of these figures and the d-vacancy count used in Fig. 14 such that the structures common to the three classes of alloys can be placed on a common map. Johannes et al. have (38) made band theory estimates of the relative energies of these MM_2 Laves structures and have shown at the C15 is indeed expected to be stable relative to the C14 in two such regions. Also, the Laves structures are seen to prefer negative $\Delta\phi$, whatever the atomic constituents (compare with Figs. 9 and 11).

As can be seen from the map, the σ phases have vacancy numbers extending from 2.95 to 5.7. Except for the $CaCu_5$ which is the least closely related, all the structurally related phases fall in the same region. While only modest separation is obtained with this parameter alone, considerable orderliness is obtained upon using the pair. Most maps involving structure, solubility or other properties, such as Figs. 8 to 11 in this review, are used to separate systems which are generally quite different from one another. Here the separation is among systems which are very much alike and the mapping still works.

Summary

Many sets of parameters are employed in the various models of alloy and compound formation. As we have tried to indicate, questions arise concerning the interrelationships between parameters which, unfortunately, are not linearly independent of one another. In general it is also impossible to provide a unique definition of some "physical" parameter. The electronegativity parameter has been used as an example of such problems. ϕ scales have bbeen defined in a variety of ways and the extent to which the results are alike is surprising. However, there are differences and they are of significance to the predictions employing the ϕ. St. John and Bloch's scale (16) which incorporates effective radii based on a pseudopotential analysis of ionization energies, was compared with a Mulliken scale based on the ionization energies directly. Subtle, valence dependent, differences were seen. In fact, the discrepancies are greater than those between the Mulliken and

Pauling scales for the main group elements. The respective roles of size, for example radii, and energy remain to be disentangled. The ϕ scales based on such quantities provide a measure of the availability, in some spatial or energy sense, of an electron level for charge transfer but they do not incorporate information concerning how many levels are available for such bonding. This is especially important for the transition metals which have many occupied and hole states close to the Fermi level and a model involving this is described elsewhere in these proceedings (14).

In general, a single parameter is not enough to describe alloying trends. Phillips has argued (39) that information theory indicates that two parameters provide the best basis for such schemes. There remains the question of how closely related the two parameters may be and yet usefully do this. We have considered one example of such an effort. Following Simons, St. John and Bloch we have taken two parameters, both based on ionization energies and applied them to structural maps, of binary alloys where one or both components are main group elements: the two parameters being ϕ and the s-p bonding factors. The maps show strong correlations between the structure a binary alloy assumes and the pair of parameters. The sign of the electronegativity difference was seen to be important, that is, it's important whether the majority or minority constituent of the alloy is the more electronegativity. Expressed in terms of ionization energies Simons and Blochs' s-p parameter was seen to be a variant of the familiar s-p promotion energy: established factors reappear in new guises and in new applications.

The results of Burch and coworkers (30) were seen to provide another example where the sign of the electronegativity difference is important. They considered the substitution of impurities into the Fe_3Si system which has two Fe sites. The more electronegative transition element impurities prefer one site, the more electropositive the other. Burch's results also display an interesting anticoorelation with the Darken-Gurry plots of alloy solubility described here by Gschneidner (4). The tendency for site substitution of an impurity atom which is in volume mismatch with the Fe, is enhanced if there is a substantial mismatch in their electronegativities.

It would appear that the s and p electrons of the main group elements both cooperate and compete in bonding. On the other hand, we believe the main tendency of the non-d conduction electrons in the transition elements is to screen d bonding. Instead of defining some sort of analog of the Simons-Bloch S factor, we used the d band vacancy count as the second parameter in a structural map of binary transition element alloys. Here the σ and structurally related phases were considered. Despite the close nature of the structures, including the tendency for many of the pairs of alloy constituents to form in more than one of the structures, considerable order was found in the map. As noted, there are features common to the AB_2, AM_2 and MM_2 mappings of Figs. 9, 11 and 14. It appears that there is some real or accidental correlation between the d-vacancy count and the s-p factor when applied to transition elements. This may be associated with the relationship between d-electron transfer and s-p screening raised in the discussion of

isomer shifts elsewhere in this symposium (14, 22).

Size was not explicitly introduced in the above considerations and despite the generally accepted importance of this to alloy formations, the maps were successful. Of course, in some sense, size and binding energies are inversely related to one another and hence size is implicity present in the maps. The choice of parameters employed in model schemes is based on some combination of the physical sense of the choice and the numerical success of the results (with the latter factor usually predominating). Lomer's summary at the Battelle meeting, calling for a multivarient analysis of alloy data still remains to be acted upon.

References

1. W. Hume-Rothery, Elements of Structural Metallurgy, (Institute of Metals, London, 1961); an excellent summation of the Hume-Rothery rules is given by T. R. Massalski in Physical Metallurgy, edited by R. W. Cahn (North-Holland Publishing Co., Amsterdam, 1970) p. 164 ff.

2. W. Gordy, "A New Method of Determining Electronegativity From Other Atomic Properties", Phys. Rev. 69, 604 (1946).

3. W. Pearson, "Dimensional Analysis of the Structures of Metallic Phases. A New Source of Information on the Interactions Between Atoms in the Structures of Binary Alloys", elsewhere in these proceedings.

4. K. Gschneidner, "L. S. Darken's Contributions to the Theory of Alloy Formation and Where we are Today", elsewhere in these proceedings.

5. A. R. Miedema and P. F. de Chatel, "A Semi-Empirical Approach to the Heat of Formation Problem, elsewhere in these proceedings, and references therein.

6. For a mapping of alloy solubility employing the Miedema parameters see J. R. Chelikowsky, "Solid Solubilities in Divalent Alloys", Phys. Rev. B19, 686 (1979).

7. L. Pauling, The Nature of the Chemical Bond, 3rd Ed. (Cornell University Press, Ithaca, N.Y. 1960).

8. G. Ertl in The Electron Factor in Catalysis on Metals, Editor L. H. Bennett, NBS Special Publication No. 475 [U.S. Government Printing Office, Wash., D.C. 1977]; R. Smoluchowski, "Anistropy of the Electronic Work Function of Metals", Phys. Rev. 60, 661 (1941).

9. S. Geller, "Set of Effective Coordination Number (12) Radii for the β-Wolfram Structure Elements", Acta Cryst. 9, 885 (1956).

10. R. E. Watson and L. H. Bennett in Charge Transfer/Electronic Structure of Alloys, Ed. by L. H. Bennett and R. H. Willens [Met. Soc. AIME, 1974] p. 1 "Charge Transfer in Alloys: The Blind Men and the Elephant".

11. R. E. Watson and L. H. Bennett, "A Mulliken Electronegativity Scale and the Structural Stability of Simple Compounds" J. Phys. Chem. Solids 39, 1235 (1978).

12. R. S. Mulliken, "Quelques Aspects de la Theorie des Orbitales Moleculaires", J. Chim. Phys. 46, 497 (1949).

13. C. A. Coulson, Valence, (Oxford Univ. Press, London 1952).

14. R. E. Watson and L. H. Bennett, "What's Special About Transition Metals in Alloy Phase Formation", elsewhere in these proceedings.

15. G. Simons and A. N. Bloch, "Pauli-Force Model Potential for Solids", Phys. Rev. B7, 2754 (1973); A. N. Bloch and G. Simons, "Structural Index for Elemental Solids", J. Am. Chem. Soc. 94, 8611 (1972).

16. J. St. John and A. N. Bloch, "Quantum-Defect Electronegativity Scale for Nontransition Elements", Phys. Rev. Letters 33, 1095 (1974).

17. W. M. Lomer, in Phase Stability in Metals and Alloys, ed. by P. S. Rudman, J. Stringer and R. I. Jafee (McGraw-Hill Book Co., N.Y.) 1966 p. 583.

18. See for example, J. E. Huheey "The Electronegativity of Groups", J. Phys. Chem. 69, 3284 (1964).

19. W. Gordy and W. J. Orville Thomas, "Electronegativities of the Elements", J. Chem. Phys. 24, 439 (1956).

20. J. C. Phillips, "Ionicity of the Chemical Bond in Crystals", Revs. Mod. Phys. 42, 317 (1970); "Dielectric Definition of Electronegativity" Phys. Rev. Letters 20, 550 (1968).

21. E. T. Teatum, K. A. Gschneidner, Jr. and J. T. Waber, "Compilation of Calculational Data Useful in Predicting Metallurgical Behavior of the Elements in Binary Alloy Systems". [Los Alamos Scientific Laboratory Report LA-4003] 1968 unpublished; J. T. Waber, K. Gschneidner, Jr., A. C. Larson and M. Y. Prince, Trans. The Metallurgical Society AIME 227, 717 (1963) "Prediction of Solid Solubility in Metallic Alloys".

22. R. E. Watson and L. H. Bennett, "Volume-Corrected Isomer Shifts of Transition-Metal Impurities: An Orbital Electronegativity Scale", Phys. Rev. B15, 5136 (1977); "Comment on Volume-Corrected Isomer Shifts of Transition-Metal Impurities", Phys. Rev. B17, 3714 (1978).

23. J. R. Chelikowsky and M. L. Cohen, "Nonlocal Pseudopotential Calculations for the Electronic Structure of Eleven Diamond and Zinc-Blende Seminconductors", Phys. Rev. B14, 556 (1976).

24. W. Andreoni, A. Baldereschi, F. Meloni and J. C. Phillips, "Renormalized Orbital Radii", Solid. State Comm. 25, 245 (1978).

25. E. S. Machlin, T. P. Chow and J. C. Phillips, "Structural Stability of Suboctet Simple Binary Compounds", Phys. Rev. Letters 38, 1292 (1977).

26. Landolt-Börnstein New Series, Structure Data of Elements and Intermetallic Phases, (Edited by K.-H. Hellwege and A. M. Hellwege), Vol. 6. Springer-Verlag, Heidelberg (1971).

27. I. D. Weisman, L. J. Swartzendruber and L. H. Bennett, Chap. 9 "Nuclear Resonances in Metals: Nuclear Magnetic Resonance and Mossbauer Effect" in Techniques in Metals Research, Vol. 6 part 2, Edited by R. F. Bunshah (John Wiley, New York, 1973). See Figure 8, page 191 for suitable Mössbauer isotopes.

28. T. K. Sham, M. L. Perlman and R. E. Watson, Phys. Rev. B (to appear in 1979).

29. R. Hultgren, P. Desai, D. T. Hawkins, M. Gleiser and K. K. Kelly, "Selected Values of the Thermodynamic Properties of Binary Alloys" (Am. Soc. for Metals, Metals Park, Ohio 1973).

30. T. J. Burch, J. I. Budnick, V. Niculesca, K. Raj, and T. Litrenta (to be published).

31. R. E. Watson and L. H. Bennett, "Transition Metals: d-Hybridization, Electronegativities and Structural Stability of Intermetallic Compounds", Phys. Rev. B 18, 6439 (1978).

32. R. E. Watson and L. H. Bennett, "Electron Factors in the Occurrence of Sigma and Structurally Related Transition Metal Alloy Phases", Scripta Metallurgica 12, 1165 (1978).

33. C. P. Shoemaker and D. P. Shoemaker in Development in the Structural Chemistry of Alloy Phases, edited by B. C. Giessen (Plenum Press, New York, 1969) p. 107.

34. M. V. Nevitt in Electronic Structure and Alloy Chemistry of the Transition Elements, edited by P. A. Beck (John Wiley and Sons, New York, 1963) p. 101.

35. W. Hume-Rothery, The Structures of Alloys of Iron (Pergamon Press, London, 1966).

36. E. O. Hall and S. H. Algie, "The Sigma Phase", Metallurgical Reviews 11, 61 (1966).

37. J. H. Wernick in Intermetallic Compounds, edited by J. H. Westbrook (John Wiley and Sons, New York, 1967) p. 197.

38. R. L. Johannes, R. Haydock, and V. Heine, "Phase Stability in Transition-Metal Laves Phases", Phys. Rev. Letters 36, 372 (1976).

39. J. R. Chelikowsky and J. C. Phillips, "Quantum-Defect Theory of Heats of Formation and Structural Transition Energies of Liquid and Solid Simple Metal Alloys and Compounds", Phys. Rev. B17, 2453 (1978).